Received: 16 May 2023 | Revised: 31 May 2023 | Accepted: 6 June 2023

DOI: 10.1002/pip.3726

SHORT COMMUNICATION

PROGRESS IN PHOTOVOLTAICS WILEY

Solar cell efficiency tables (version 62)

Martin A. Green[1] | Ewan D. Dunlop[2] | Masahiro Yoshita[3] | Nikos Kopidakis[4] | Karsten Bothe[5] | Gerald Siefer[6] | Xiaojing Hao[1]

[1]Australian Centre for Advanced Photovoltaics, School of Photovoltaic and Renewable Energy Engineering, University of New South Wales, Sydney, Australia

[2]European Commission–Joint Research Centre, Ispra, Varese, Italy

[3]Renewable Energy Research Center (RENRC), National Institute of Advanced Industrial Science and Technology (AIST), Central 2, Umezono 1-1-1, Tsukuba, Ibaraki, Japan

[4]National Renewable Energy Laboratory, 15013 Denver West Parkway, Golden, Colorado, USA

[5]Calibration and Test Center (CalTeC), Solar Cells Laboratory, Institut für Solarenergieforschung GmbH (ISFH), Am Ohrberg 1, Emmerthal, Germany

[6]Fraunhofer-Institute for Solar Energy Systems–ISE CalLab, Freiburg, Germany

Correspondence
Martin A. Green, School of Photovoltaic and Renewable Energy Engineering, University of New South Wales, Sydney 2052, Australia.
Email: m.green@unsw.edu.au

Funding information
U.S. Department of Energy (Office of Science, Office of Basic Energy Sciences and Energy Efficiency and Renewable Energy, Solar Energy Technology Program), Grant/Award Number: DE-AC36-08-GO28308; Australian Renewable Energy Agency (ARENA); Japanese New Energy and Industrial Technology Development Organisation (NEDO)

Abstract

Consolidated tables showing an extensive listing of the highest independently confirmed efficiencies for solar cells and modules are presented. Guidelines for inclusion of results into these tables are outlined, and new entries since January 2023 are reviewed.

KEYWORDS

energy conversion efficiency, photovoltaic efficiency, solar cell efficiency

1 | INTRODUCTION

Since January 1993, 'Progress in Photovoltaics' has published six monthly listings of the highest confirmed efficiencies for a range of photovoltaic cell and module technologies.[1–3] By providing guidelines for the inclusion of results into these tables, this not only provides an authoritative summary of the current state-of-the-art but also encourages researchers to seek independent confirmation of results and to report results on a standardised basis. In version 33 of these tables,[3] results were updated to the new internationally accepted reference spectrum (International Electrotechnical Commission IEC 60904-3, Ed. 2, 2008).

The most important criterion for the inclusion of results into the tables is that they must have been independently measured by a recognised test centre listed elsewhere[1] (an additional test centre listed in Appendix A). A distinction is made between three different

TABLE 1 Confirmed single-junction terrestrial cell and submodule efficiencies measured under the global AM1.5 spectrum (1000 W/m^2) at 25°C (IEC 60904-3: 2008 or ASTM G-173-03 global).

Classification	Efficiency (%)	Area (cm^2)	V_{oc} (V)	J_{sc} (mA/cm^2)	Fill factor (%)	Test centre (date)	Description
Silicon							
Si (crystalline cell)	26.8 ± 0.4[a]	274.4 (t)	0.7514	41.45[b]	86.1	ISFH (10/22)	LONGi, n-type HJT[4]
Si (DS wafer cell)	24.4 ± 0.3[a]	267.5 (t)	0.7132	41.47[c]	82.5	ISFH (8/20)	Jinko Solar, n-type
Si (thin transfer submodule)	21.2 ± 0.4	239.7 (ap)	0.687[e]	38.50[d,e]	80.3	NREL (4/14)	Solexel (35 μm thick)[5]
Si (thin-film minimodule)	10.5 ± 0.3	94.0 (ap)	0.492[e]	29.7[d,f]	72.1	FhG-ISE (8/07)	CSG Solar (<2 μm on glass)[6]
III–V cells							
GaAs (thin-film cell)	29.1 ± 0.6	0.998 (ap)	1.1272	29.78[g]	86.7	FhG-ISE (10/18)	Alta Devices[7]
GaAs (multicrystalline)	18.4 ± 0.5	4.011 (t)	0.994	23.2	79.7	NREL (11/95)	RTI, Ge substrate[8]
InP (crystalline cell)	24.2 ± 0.5[h]	1.008 (ap)	0.939	31.15[i]	82.6	NREL (3/13)	NREL[9]
Thin-film chalcogenide							
CIGS (cell) (Cd-free)	23.35 ± 0.5	1.043 (da)	0.734	39.58[j]	80.4	AIST (11/18)	Solar Frontier[10]
CIGSSe (submodule)	**20.3 ± 0.4**	**526.7 (ap)**	**0.6834**	**39.55[dk]**	**75.1**	**NREL (5/23)**	**Avancis, 100 cells[11]**
CdTe (cell)	21.0 ± 0.4	1.0623 (ap)	0.8759	30.25[e]	79.4	Newport (8/14)	First Solar, on glass[12]
CZTSSe (cell)	**12.1 ± 0.3**	**1.066 (da)**	**0.5379**	**35.29[k]**	**63.6**	**NPVM (4/23)**	**IoP/CAS[13]**
CZTS (cell)	10.0 ± 0.2	1.113 (da)	0.7083	21.77[i]	65.1	NREL (3/17)	UNSW[14]
Amorphous/microcrystalline							
Si (amorphous cell)	10.2 ± 0.3[l,h]	1.001 (da)	0.896	16.36[e]	69.8	AIST (7/14)	AIST[15]
Si (microcrystalline cell)	11.9 ± 0.3[h]	1.044 (da)	0.550	29.72[i]	75.0	AIST (2/17)	AIST[16]
Perovskite							
Perovskite (cell)	**24.35 ± 0.5[m]**	**1.007 (da)**	**1.159**	**25.60[k]**	**82.1**	**NPVM (4/23)**	**NUS/SERIS[17]**
Perovskite (minimodule)	22.4 ± 0.5[m]	26.02 (da)	1.127[d]	25.61[d,b]	77.6	NPVM (7/22)	EPFLSion/NCEPU, 8 cells[18]
Dye sensitised							
Dye (cell)	11.9 ± 0.4[n]	1.005 (da)	0.744	22.47[o]	71.2	AIST (9/12)	Sharp[19,20]
Dye (minimodule)	10.7 ± 0.4[n]	26.55 (da)	0.754[d]	20.19[d,p]	69.9	AIST (2/15)	Sharp, 7 serial cells[19,20]
Dye (submodule)	8.8 ± 0.3[n]	398.8 (da)	0.697[d]	18.42[d,q]	68.7	AIST (9/12)	Sharp, 26 serial cells[19,20]
Organic							
Organic (cell)	15.2 ± 0.2[h,r]	1.015 (da)	0.8467	24.24[c]	74.3	FhG-ISE (10/20)	Fraunhofer ISE[21]
Organic (minimodule)	**15.7 ± 0.3[r]**	**19.31 (da)**	**0.8771[d]**	**24.37[el]**	**73.4**	**JET (1/23)**	**ZhejiangU, 7 cells[22]**
Organic (submodule)	11.7 ± 0.2[r]	203.98 (da)	0.8177[d]	20.68[d,s]	69.3	FhG-ISE (10/19)	ZAE Bayern, 33 cells[23]

Abbreviations: (ap), aperture area; (da), designated illumination area; (t), total area; AIST; Japanese National Institute of Advanced Industrial Science and Technology; a-Si, amorphous silicon/hydrogen alloy; CIGS, $CuIn_{1-y}Ga_ySe_2$; CZTS, Cu_2ZnSnS_4; CZTSSe, $Cu_2ZnSnS_{4-y}Se_y$; DS, directionally solidified (including mono cast and multicrystalline); FhG-ISE, Fraunhofer Institut für Solare Energiesysteme; nc-Si, nanocrystalline or microcrystalline silicon.

[a]Contacting: Front: 9BB, busbar resistance neglecting; Rear: 9BB, full area contacting, highly reflective chuck.
[b]Spectral response and current–voltage curve reported in version 61 of these tables.
[c]Spectral response and current–voltage curve reported in version 57 of these tables.
[d]Reported on a 'per cell' basis.
[e]Spectral responses and current–voltage curve reported in version 45 of these tables.
[f]Recalibrated from original measurement.
[g]Spectral response and current–voltage curve reported in version 53 of these tables.
[h]Not measured at an external laboratory.
[i]Spectral response and current–voltage curve reported in version 50 of these tables.
[j]Spectral response and current–voltage curve reported in version 54 of these tables.
[k]Spectral response and current–voltage curve reported in the present version of these tables.
[l]Stabilised by 1000-h exposure to 1 sunlight at 50°C.
[m]Initial performance. References 24 and 25 review the stability of similar devices.
[n]Initial efficiency. Reference 26 reviews the stability of similar devices.
[o]Spectral response and current–voltage curve reported in version 41 of these tables.
[p]Spectral response and current–voltage curve reported in version 46 of these tables.
[q]Spectral response and current–voltage curve reported in version 43 of these tables.
[r]Initial performance. References 27 and 28 review the stability of similar devices.
[s]Spectral response and current–voltage curve reported in version 55 of these tables.

PROGRESS IN PHOTOVOLTAICS – WILEY

eligible definitions of cell area: total area, aperture area and designated illumination area, as also defined elsewhere[1] (note that, if masking is used, masks must have a simple aperture geometry, such as square, rectangular or circular—masks with multiple openings are not eligible). 'Active area' efficiencies are not included. There are also certain minimum values of the area sought for the different device types (above 0.05 cm^2 for a concentrator cell, 1 cm^2 for a one-sun cell, 200 cm^2 for a 'submodule' and 800 cm^2 for a module).

In recent years, approaches for contacting large-area solar cells during measurement have become increasingly complex. Since there is no explicit standard for the design of solar cell contacting units, in an earlier issue,[2] we describe approaches for temporary electrical contacting of large-area solar cells both with and without busbars. To enable comparability between different contacting approaches and to clarify the corresponding measurement conditions, an unambiguous denotation was introduced and used in subsequent versions of these tables.

TABLE 2 'Notable exceptions' for single-junction cells and submodules: 'top dozen' confirmed results, not class records, measured under the global AM1.5 spectrum (1000 Wm^{-2}) at 25°C (IEC 60904-3: 2008 or ASTM G-173-03 global).

Classification	Efficiency (%)	Area (cm^2)	V_{oc} (V)	J_{sc} (mA/cm^2)	Fill factor (%)	Test centre (date)	Description
Cells (silicon)							
Si (crystalline)	25.0 ± 0.5	4.00 (da)	0.706	42.7[a]	82.8	Sandia (3/99)	UNSW, p-type PERC[29]
Si (crystalline)	25.8 ± 0.5[b]	4.008 (da)	0.7241	42.87[c]	83.1	FhG-ISE (7/17)	FhG-ISE, n-type TOPCon[30]
Si (crystalline)	26.0 ± 0.5[b]	4.015 (da)	0.7323	42.05[d]	84.3	FhG-ISE (11/19)	FhG-ISE, p-type TOPCon
Si (crystalline)	26.7 ± 0.5	79.0 (da)	0.738	42.65[a]	84.9	AIST (3/17)	Kaneka, n-type rear IBC[31]
Si (crystalline)	26.1 ± 0.3[b]	3.9857 (da)	0.7266	42.62[e]	84.3	ISFH (2/18)	ISFH, p-type rear IBC[32]
Si (large)	24.0 ± 0.3[f]	244.59 (t)	0.6940	41.58[g]	83.3	ISFH (7/19)	LONGi, p-type PERC[33]
Si (large)	25.3 ± 0.4[h]	268.0 (t)	0.7214	42.07[i]	83.4	ISFH (11/21)	Jinko, n-type TOPCon[34]
Si (large)	26.6 ± 0.4[j]	274.1 (t)	0.7513	41.30	85.6	ISFH (10/22)	LONGi, p-type HJT[35]
Si (large)	26.6 ± 0.5	179.74 (da)	0.7403	42.5[k]	84.7	FhG-ISE (11/16)	Kaneka, n-type rear IBC[31]
Cells (III–V)							
GaInP	22.0 ± 0.3[b]	0.2502 (ap)	1.4695	16.63[l]	90.2	NREL (1/19)	NREL, rear HJ, strained AlInP[36]
Cells (chalcogenide)							
CIGS (thin-film)	**23.6 ± 0.4**	**0.899 (da**	**0.7671**	**38.30**[m]	**80.5**	**FhG-ISE (1/23)**	**Evolar/UppsalaU**[37]
CdTe (thin-film)	**22.3 ± 0.2**	**0.4491 (da)**	**0.8985**	**31.69**[m]	**78.9**	**NREL (2/23)**	**First Solar**[38]
CZTSSe (thin-film)	**14.9 ± 0.3**	**0.2694 (da)**	**0.5554**	**36.93**[m]	**72.5**	**NPVM (4/23)**	**IoP/CAS**[13]
CZTS (thin-film)	**11.4 ± 0.3**	**0.2039 (da)**	**0.7458**	**21.79**[m]	**69.9**	**NPVM (5/23)**	**UNSW (Cd-free)**[39]
Cells (other)							
Perovskite (thin-film)	**26.0 ± 0.5**[n,o]	**0.07461 (da)**	**1.190**	**26.00**[m]	**84.0**	**JET (3/23)**	**IoS/CAS**[40]
Organic (thin-film)	**19.2 ± 0.3**[p]	**0.0326 (da)**	**0.9135**	**26.61**[m]	**79.0**	**NREL (3/23)**	**SJTU**[41]
Dye sensitised	**13.0 ± 0.4**[q]	**0.1155 (da)**	**1.0396**	**15.55**[m]	**80.4**	**FhG-ISE (10/20)**	**EPFL**[42]

Abbreviations: (ap), aperture area; (da), designated illumination area; (t), total area; AIST, Japanese National Institute of Advanced Industrial Science and Technology; CIGS, $CuIn_{1-y}Ga_ySe_2$; CZTS, Cu_2ZnSnS_4; CZTSSe, $Cu_2ZnSnS_{4-y}Se_y$; FhG-ISE, Fraunhofer-Institut für Solare Energiesysteme; ISFH, Institute for Solar Energy Research, Hamelin; NREL, National Renewable Energy Laboratory.

[a]Spectral response reported in version 36 of these tables.
[b]Not measured at an external laboratory.
[c]Spectral response and current–voltage curves reported in version 51 of these tables.
[d]Spectral response and current–voltage curves reported in version 55 of these tables.
[e]Spectral response and current–voltage curve reported in version 52 of these tables.
[f]Contacting: Front: 12BB, busbar resistance neglected; Rear: fully metallized, full area contacting.
[g]Spectral response and current–voltage curves reported in version 57 of these tables.
[h]Contacting: Front: 0BB, grid resistance neglecting; Rear: 9BB, full area contacting, highly reflective chuck.
[i]Spectral response and current–voltage curves reported in version 60 of these tables.
[j]Contacting: Front: busbar resistance neglecting contacting; Rear: 9BB, grid resistance neglecting contacting, gold plated chuck.
[k]Spectral response and current–voltage curves reported in version 50 of these tables.
[l]Spectral response and current–voltage curve reported in version 54 of these tables.
[m]Spectral response and current–voltage curves reported in the present version of these tables.
[n]Stability not investigated. References 24 and 25 document stability of similar devices.
[o]Measured using 10-point IV sweep with constant voltage bias until current change rate <0.07%/min.
[p]Long-term stability not investigated. References 27 and 28 document stability of similar devices.
[q]Long-term stability not investigated. Reference 26 documents stability of similar devices.

TABLE 3 Confirmed multiple-junction terrestrial cell and submodule efficiencies measured under the global AM1.5 spectrum (1000 W/m^2) at 25°C (IEC 60904-3: 2008 or ASTM G-173-03 global).

Classification	Efficiency (%)	Area (cm^2)	V_{oc} (V)	J_{sc} (mA/cm^2)	Fill factor (%)	Test centre (date)	Description
III–V multijunctions							
5 junction cell (bonded) (2.17/1.68/1.40/1.06/.73 eV)	38.8 ± 1.2	1.021 (ap)	4.767	9.564	85.2	NREL (7/13)	Spectrolab, 2-terminal
InGaP/GaAs/InGaAs	37.9 ± 1.2	1.047 (ap)	3.065	14.27[a]	86.7	AIST (2/13)	Sharp, 2-term.[43]
GaInP/GaAs (monolithic)	32.8 ± 1.4	1.000 (ap)	2.568	14.56[b]	87.7	NREL (9/17)	LG Electronics, 2-term.
III–V/Si multijunctions							
GaInP/GaInAsP/Si (bonded)	35.9 ± 1.3[c]	3.987 (ap)	3.248	13.11[d]	84.3	FhG-ISE (4/20)	Fraunhofer ISE, 2-term.[44]
GaInP/GaAs/Si (mech. stack)	35.9 ± 0.5[c]	1.002 (da)	2.52/0.681	13.6/11.0	87.5/78.5	NREL (2/17)	NREL/CSEM/EPFL, 4-term.[45]
GaInP/GaAs/Si (monolithic)	25.9 ± 0.9[c]	3.987 (ap)	2.647	12.21[e]	80.2	FhG-ISE (6/20)	Fraunhofer ISE, 2-term.[46]
GaAsP/Si (monolithic)	23.4 ± 0.3	1.026 (ap)	1.732	17.34[f]	77.7	NREL (5/20)	OSU/UNSW/SolAero, 2-term.[47]
GaAs/Si (mech. stack)	32.8 ± 0.5[c]	1.003 (da)	1.09/0.683	28.9/11.1[g]	85.0/79.2	NREL (12/16)	NREL/CSEM/EPFL, 4-term.[45]
GaInP/GaInAs/Ge; Si (spectral split minimodule)	34.5 ± 2.0	27.83 (ap)	2.66/0.65	13.1/9.3	85.6/79.0	NREL (4/16)	UNSW/Azur/Trina, 4-term.[48]
Perov./Si multijunctions							
Perovskite/Si	**33.7 ± 1.1**[h]	**1.0035 (da)**	**1.974**	**20.99**[i]	**81.3**	**JRC/ESTI (5/23)**	**KAUST, 2-term.**[49]
Perovskite/Si (large)	**28.6 ± 1.4**[h]	**258.14 (t)**	**1.909**	**19.11**[i]	**78.3**	**FhG-ISE (5/23)**	**Oxford PV, 2-term.**[50]
Perov.(minimod.)/Si (cell)	**28.4 ± 0.7**[h]	**63.98 (da)**	**1.21**[j]**/.648**	**21.9**[ij]**/14.3**	**78.7/81.4**	**AIST (1/23)**	**Kaneka, 4-term.**[51]
Other multijunctions							
Perovskite/CIGS	24.2 ± 0.7[h]	1.045 (da)	1.768	19.24[f]	72.9	FhG-ISE (1/20)	HZB, 2-terminal[52]
Perovskite/perovskite	**28.2 ± 0.5**[h]	**1.038 (da)**	**2.159**	**16.59**[i]	**78.9**	**JET (12/22)**	**NanjingU/Renshine, 2-term.**[53]
Perovskite/perovskite (minimodule)	24.5 ± 0.6[h]	20.25 (da)	2.157	14.86[k]	77.5	JET (6/22)	NanjingU/Renshine, 2-term.[54]
a-Si/nc-Si/nc-Si (thin-film)	14.0 ± 0.4[l,c]	1.045 (da)	1.922	9.94[m]	73.4	AIST (5/16)	AIST, 2-term.[55]
a-Si/nc-Si (thin-film cell)	12.7 ± 0.4[l,c]	1.000 (da)	1.342	13.45[n]	70.2	AIST (10/14)	AIST, 2-term.[56]
'Notable exceptions'							
GaInP/GaAs (mqw)	32.9 ± 0.5[c]	0.250 (ap)	2.500	15.36[o]	85.7	NREL (1/20)	NREL/UNSW, multiple QW
GaInP/GaAs/GaInAs	37.8 ± 1.4	0.998 (ap)	3.013	14.60[o]	85.8	NREL (1/18)	Microlink (ELO)[57]
GaInP/GaAs (mqw)/GaInAs	39.5 ± 0.5[c]	0.242 (ap)	2.997	15.44[p]	85.3	NREL (9/21)	NREL, multiple QW
6 junction (monolithic) (2.19/1.76/1.45/1.19/.97/.7 eV)	39.2 ± 3.2[c]	0.247 (ap)	5.549	8.457[q]	83.5	NREL (11/18)	NREL, inv. metamorphic[58]
GaInP/AlGaAs/CIGS	28.1 ± 1.2[c]	0.1386 (da)	2.952	11.72[d]	81.1	AIST (1/21)	AIST/FhG-ISE, 2-term.[59]
Perovskite/perovskite	**29.1 ± 0.5**[h]	**0.0489 (da)**	**2.154**	**16.51**[i]	**81.7**	**JET (12/22)**	**NanjingU/Renshine, 2-term.**[53]
Perovskite/organic	23.4 ± 0.8[h]	0.0552 (da)	2.136	14.56[r]	75.6	JET (3/22)	NUS/SERIS, 2-term.[60]

Abbreviations: (ap), aperture area; (da), designated illumination area; (t), total area; AIST, Japanese National Institute of Advanced Industrial Science and Technology; a-Si, amorphous silicon/hydrogen alloy; FhG-ISE, Fraunhofer Institut für Solare Energiesysteme; nc-Si, nanocrystalline or microcrystalline silicon.
[a]Spectral response and current–voltage curve reported in version 42 of these tables.
[b]Spectral response and current–voltage curve reported in the version 51 of these tables.
[c]Not measured at an external laboratory.
[d]Spectral response and current–voltage curve reported in version 58 of these tables.
[e]Spectral response and current–voltage curve reported in version 57 of these tables.
[f]Spectral response and current–voltage curve reported in version 56 of these tables.
[g]Spectral response and current–voltage curve reported in version 52 of these tables.
[h]Initial efficiency. References 24 and 25 review the stability of similar perovskite-based devices.
[i]Spectral response and current–voltage curves reported in the present version of these tables.
[j]Reported on a 'per cell' basis.
[k]Spectral response and current–voltage curve reported in version 61 of these tables.
[l]Stabilised by 1000-h exposure to 1 sunlight at 50°C.
[m]Spectral response and current–voltage curve reported in version 49 of these tables.
[n]Spectral responses and current–voltage curve reported in version 45 of these tables.
[o]Spectral response and current–voltage curve reported in version 53 of these tables.
[p]Spectral response and current–voltage curves reported in version 59 of these tables.
[q]Spectral response and current–voltage curve reported in version 54 of these tables.
[r]Spectral response and current–voltage curve reported in version 60 of these tables.

TABLE 4 Confirmed non-concentrating terrestrial module efficiencies measured under the global AM1.5 spectrum (1000 W/m^2) at a cell temperature of 25°C (IEC 60904-3: 2008 or ASTM G-173-03 global).

Classification	Effic. (%)	Area (cm^2)	V_{oc} (V)	I_{sc} (A)	FF (%)	Test centre (date)	Description
Si (crystalline)	**24.7 ± 0.3**	**17,806 (da)**	**83.04**	**6.384[a]**	**82.9**	**NREL (4/23)**	**Maxeon (112 cells)**
Si (multicrystalline)	20.4 ± 0.3	14,818 (ap)	39.90	9.833[b]	77.2	FhG-ISE (10/19)	Hanwha Q Cells (60 cells)[61]
GaAs (thin-film)	25.1 ± 0.8	866.45 (ap)	11.08	2.303[c]	85.3	FhG-ISE (11/17)	Alta Devices[62]
CIGS (Cd-free)	19.2 ± 0.5	841 (ap)	48.0	0.456[c]	73.7	AIST (1/17)	Solar Frontier (70 cells)[63]
CdTe (thin-film)	19.5 ± 1.4	23,582 (da)	227.9	2.622[d]	76.8	NREL (9/21)	First Solar[64]
a-Si/nc-Si (tandem)	12.3 ± 0.3[e]	14,322 (t)	280.1	0.902[f]	69.9	ESTI (9/14)	TEL Solar, Trubbach Labs[65]
Perovskite	**18.6 ± 0.7[g]**	**809.9 (da)**	**44.7**	**0.479[a]**	**70.3**	**JET (5/23)**	**UtmoLight (39 cells)[66]**
Organic	13.1 ± 0.3[h]	1,475.0 (da)	48.10	0.6015[a]	67.8	NREL (5/23)	Ways/Nanobit[67]
Multijunction							
InGaP/GaAs/InGaAs	32.65 ± 0.7	965 (da)	24.30	1.520[d]	85.3	AIST (2/22)	Sharp (40 cells; 8 series)[68]
'Notable Exceptions'							
CIGS (large)	18.6 ± 0.6	10,858 (ap)	58.00	4.545[b]	76.8	FhG-ISE (10/19)	Miasole[69]
InGaP/GaAs//Si	**33.7 ± 0.7**	**775 (da)**	**20.3/2.83**	**1.25/1.93[a]**	**86.5/78.0**	**AIST (2/23)**	**Sharp, 4-term.[70]**
InGaP/GaAs//CIGS	**31.2 ± 0.7**	**778 (ap)**	**20.3/16.9**	**1.24/.26[a]**	**85.7/59.8**	**AIST (2/23)**	**Sharp, 4-term.[70]**

Abbreviations: (ap), aperture area; (da), designated illumination area; (t), total area; a-Si, amorphous silicon/hydrogen alloy; a-SiGe, amorphous silicon/germanium/hydrogen alloy; CIGSS, CuInGaSSe; Effic, efficiency; FF, fill factor; nc-Si, nanocrystalline or microcrystalline silicon.
[a]Spectral response and current–voltage curve reported in the present version of these tables.
[b]Spectral response and current–voltage curve reported in version 55 of these tables.
[c]Spectral response and current–voltage curve reported in version 50 or 51 of these tables.
[d]Spectral response and current–voltage curve reported in version 60 of these tables.
[e]Stabilised at the manufacturer to the 2% level following IEC procedure of repeated measurements.
[f]Spectral response and/or current–voltage curve reported in version 46 of these tables.
[g]Initial performance. References 25 and 26 review the stability of similar devices.
[h]Initial performance. References 28 and 29 review the stability of similar devices.

Tabled results are reported for cells and modules made from different semiconductors and for sub-categories within each semiconductor grouping (e.g., crystalline, polycrystalline or directionally solidified and thin film). From version 36 onwards, spectral response information is included (when possible) in the form of a plot of the external quantum efficiency (EQE) versus wavelength, either as

TABLE 5 Terrestrial concentrator cell and module efficiencies measured under the ASTM G-173-03 direct beam AM1.5 spectrum at a cell temperature of 25°C (except where noted for the hybrid and luminescent modules).

Classification	Effic. (%)	Area (cm^2)	Intensity[a] (suns)	Test centre (date)	Description
Single cells					
GaAs	30.8 ± 1.9[b,c]	0.0990 (da)	61	NREL (1/22)	NREL, 1 junction (1J)
Si	27.6 ± 1.2[d]	1.00 (da)	92	FhG-ISE (11/04)	Amonix back-contact[71]
CIGS (thin-film)	23.3 ± 1.2[b,e]	0.09902 (ap)	15	NREL (3/14)	NREL[72]
Multijunction cells					
AlGaInP/AlGaAs/GaAs/GaInAs(3) (2.15/1.72/1.41/1.17/0.96/0.70 eV)	47.1 ± 2.6[b,f]	0.099 (da)	143	NREL (3/19)	NREL, 6J inv. metamorphic[58]
GaInP/GaInAs; GaInAsP/GaInAs	47.6 ± 2.6[b,g]	0.0452 (da)	665	FhG-ISE (5/22)	FhG-ISE 4J bonded[73]
GaInP/GaAs/GaInAs/GaInAs	45.7 ± 2.3[b,h]	0.09709 (da)	234	NREL (9/14)	NREL, 4J monolithic[74]
InGaP/GaAs/InGaAs	44.4 ± 2.6[i]	0.1652 (da)	302	FhG-ISE (4/13)	Sharp, 3J inverted metamorphic[75]
GaInAsP/GaInAs	35.5 ± 1.2[b,j]	0.10031 (da)	38	NREL (10/17)	NREL 2-junction (2 J)[76]
Minimodule					
GaInP/GaAs; GaInAsP/GaInAs	43.4 ± 2.4[b,k]	18.2 (ap)	340[l]	FhG-ISE (7/15)	Fraunhofer ISE 4J (lens/cell)[77]
Submodule					
GaInP/GaInAs/Ge; Si	40.6 ± 2.0[k]	287 (ap)	365	NREL (4/16)	UNSW 4J split spectrum[78]
Modules					
Si	20.5 ± 0.8[b]	1875 (ap)	79	Sandia (4/89)[l]	Sandia/UNSW/ENTECH (12 cells)[79]
Three junction (3J)	35.9 ± 1.8[m]	1,092 (ap)	N/A	NREL (8/13)	Amonix[80]
Four junction (4J)	38.9 ± 2.5[n]	812.3 (ap)	333	FhG-ISE (4/15)	Soitec[81]
Hybrid module[o]					
4-Junction (4J)/bifacial c-Si	34.2 ± 1.9[b,o]	1,088 (ap)	CPV/PV	FhG-ISE (9/19)	FhG-ISE (48/8 cells; 4T)[82]
'Notable exceptions'					
Si (large area)	21.7 ± 0.7	20.0 (da)	11	Sandia (9/90)[l]	UNSW laser grooved[83]
Luminescent Minimodule[o]	7.1 ± 0.2	25 (ap)	2.5[p]	ESTI (9/08)	ECN Petten, GaAs cells[84]
4J Minimodule	41.4 ± 2.6[b]	121.8 (ap)	230	FhG-ISE (9/18)	FhG-ISE, 10 cells[85]

Note: Following the normal convention, efficiencies calculated under this direct beam spectrum neglect the diffuse sunlight component that would accompany this direct spectrum. These direct beam efficiencies need to be multiplied by a factor estimated as 0.8746 to convert to thermodynamic efficiencies.[86]

Abbreviations: (ap), aperture area; (da), designated illumination area; CIGS, $CuInGaSe_2$; Effic, efficiency; FhG-ISE, Fraunhofer-Institut für Solare Energiesysteme; NREL, National Renewable Energy Laboratory.

[a]One sun corresponds to direct irradiance of 1000 Wm^{-2}.
[b]Not measured at an external laboratory.
[c]Spectral response and current–voltage curve reported in version 60 of these tables.
[d]Measured under a low aerosol optical depth spectrum similar to ASTM G-173-03 direct.[87]
[e]Spectral response and current–voltage curve reported in version 44 of these tables.
[f]Spectral response and current–voltage curve reported in version 54 of these tables.
[g]Spectral response and current–voltage curve reported in version 61 of these tables.
[h]Spectral response and current–voltage curve reported in version 46 of these tables.
[i]Spectral response and current–voltage curve reported in version 42 of these tables.
[j]Spectral response and current–voltage curve reported in version 51 of these tables.
[k]Determined at IEC 62670-1 CSTC reference conditions.
[l]Recalibrated from original measurement.
[m]Referenced to 1000-W/m^2 direct irradiance and 25°C cell temperature using the prevailing solar spectrum and an in-house procedure for temperature translation.
[n]Measured under IEC 62670-1 reference conditions following the current IEC power rating draft 62670-3.
[o]Thermodynamic efficiency. Hybrid and luminescent modules measured under the ASTM G-173-03 or IEC 60904-3: 2008 global AM1.5 spectrum at a cell temperature of 25°C.
4-terminal module with external dual-axis tracking. Power rating of CPV follows IEC 62670-3 standard, front power rating of flat plate PV based on IEC 60904-3, -5, -7, -10 and 60891 with modified current translation approach; rear power rating of flat plate PV based on IEC TS 60904-1-2 and 60891.
[p]Geometric concentration.

absolute values or normalised to the peak measured value. Current–voltage (IV) curves have also been included where possible from version 38 onwards.

The highest confirmed 'one sun' cell and module results are reported in Tables 1–4. Any changes in the tables from those previously published[1] **are set in bold type**. In most cases, a literature reference is provided that describes either the result reported, or a similar result (readers identifying improved references are welcome to submit to the lead author). Table 1 summarises the best-reported measurements for 'one-sun' (non-concentrator) single-junction cells and submodules.

Table 2 contains what might be described as 'notable exceptions' for 'one-sun' single-junction cells and submodules in the above category. While not conforming to the requirements to be recognised as a class record, the devices in Table 2 have notable characteristics that will be of interest to sections of the photovoltaic community, with entries based on their significance and timeliness. To encourage discrimination, the table is limited to nominally 12 entries with the present authors having voted for their preferences for inclusion. Readers who have suggestions of notable exceptions for inclusion into this or subsequent tables are welcome to contact any of the authors with full details. Suggestions conforming to the guidelines will be included on the voting list for a future issue.

Table 3 was first introduced in version 49 of these tables and summarises the growing number of cell and submodule results involving high efficiency, one-sun multiple-junction devices (previously

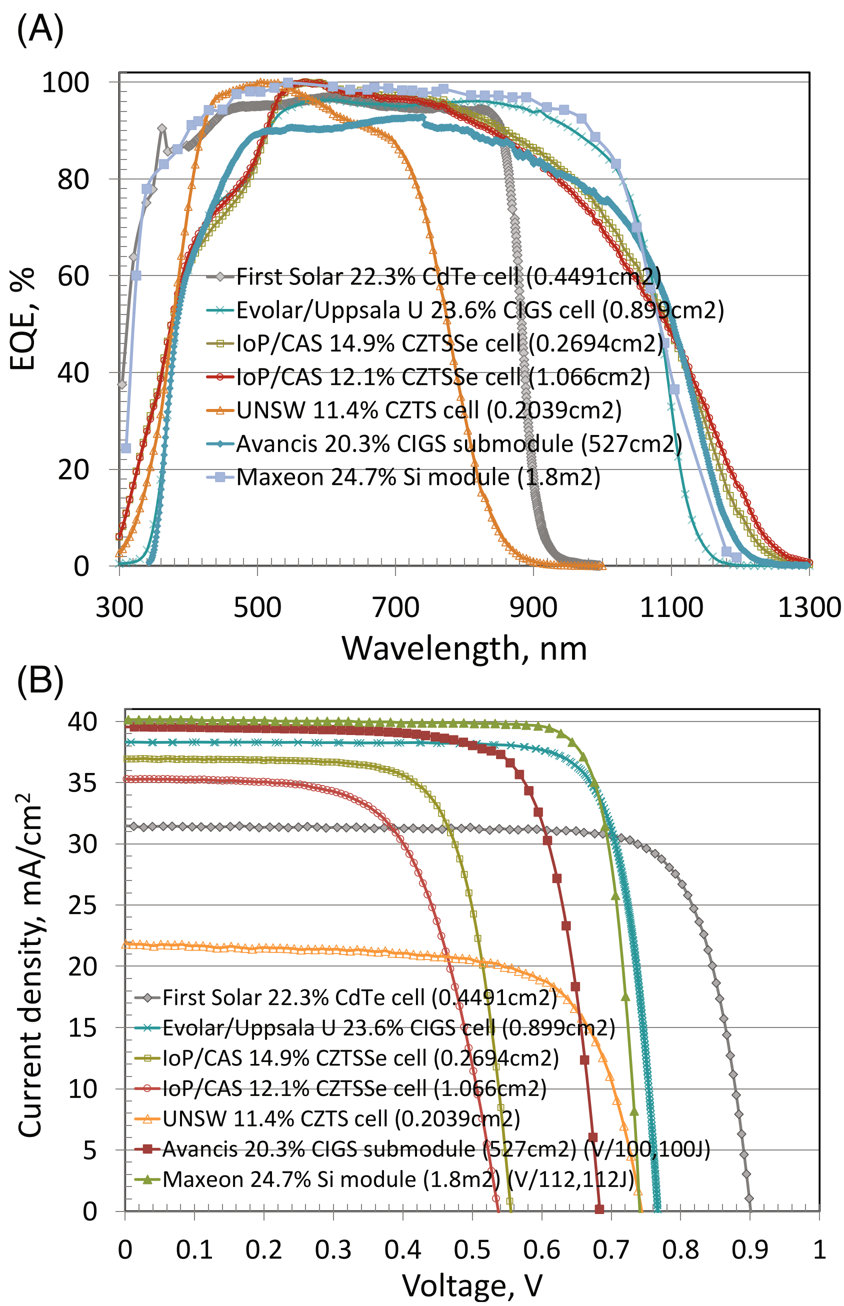

FIGURE 1 (A) External quantum efficiency (EQE) for the new chalcogenide thin-film and silicon cell and module results reported in this issue (most results are normalised). (B) Corresponding current density–voltage (JV) curves.

reported in Table 1). Table 4 shows the best results for one-sun modules, both single- and multiple-junction, while Table 5 shows the best results for concentrator cells and concentrator modules. A small number of 'notable exceptions' are also included in Tables 3 to 5.

2 | NEW RESULTS

Twenty–one new results are reported in the present version of these tables. The first new result in Table 1 ('one-sun cells and submodules') is the increase in efficiency to 20.3% for a large (527 cm^2) $CuIn_{1-x}Ga_xS_ySe_{2-y}$ (CIGSSe) submodule fabricated by Avancis[11] and measured by the US National Renewable Energy Laboratory (NREL). The second new result is 12.1% aperture area efficiency for a 1-cm^2 $Cu_2ZnSnS_ySe_{4-y}$ (CZTSSe) cell[13] fabricated by the Institute of Physics, Chinese Academy of Sciences (IoP/CAS) and measured by the Chinese National Photovoltaic Industry Measurement and Testing Center (NPVM). The third new result is 24.35% efficiency for a 1-cm^2 perovskite cell[17] fabricated by the National University of Singapore (NUS) in conjunction with the Solar Energy Research Institute of Singapore (SERIS) and again measured by NPVM. The final new result in Table 1 is 15.7% efficiency for a 19-cm^2 organic photovoltaic (OPV) minimodule[22] fabricated by Zhejiang University in collaboration with EnrichPV and Microquanta and measured by the Japan Electrical Safety and Environment Technology Laboratories (JET).

There are seven new results in Table 2 (one-sun 'notable exceptions'), all involving small area, thin-film solar cells. The first is an efficiency of 23.6% for a 0.9-cm^2 $CuIn_{1-x}Ga_xSe_2$ (CIGS) cell fabricated in a collaboration between Evolar and Uppsala University[37] and measured by the Fraunhofer Institute for Solar Energy Systems (FhG-ISE).

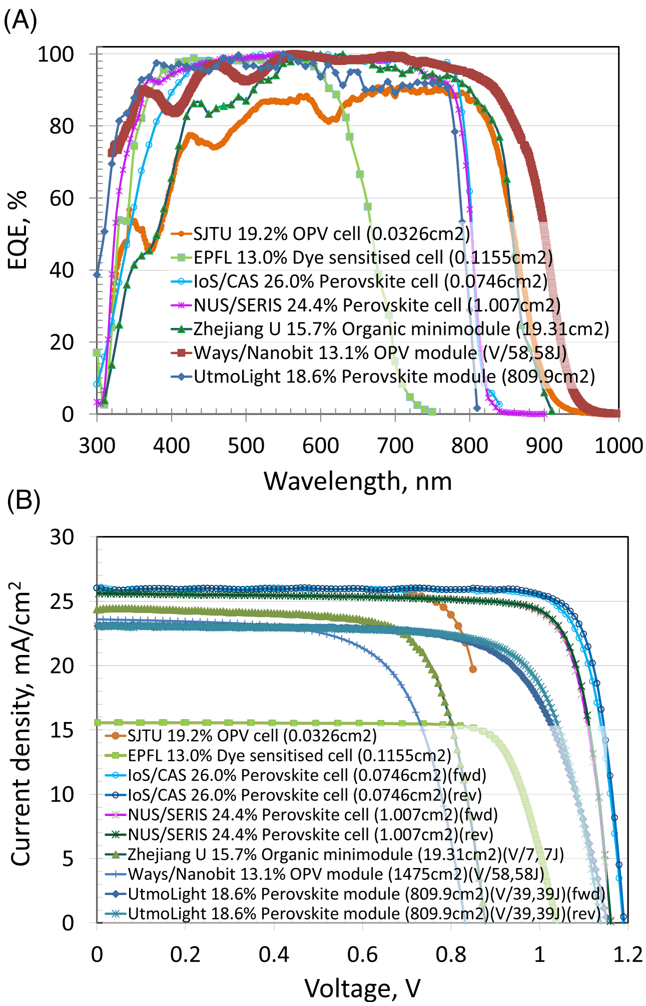

FIGURE 2 (A) External quantum efficiency (EQE) for the new perovskite, organic and dye-sensitised thin-film cell and module results reported in this issue (most results are normalised). (B) Corresponding current density–voltage (JV) curves.

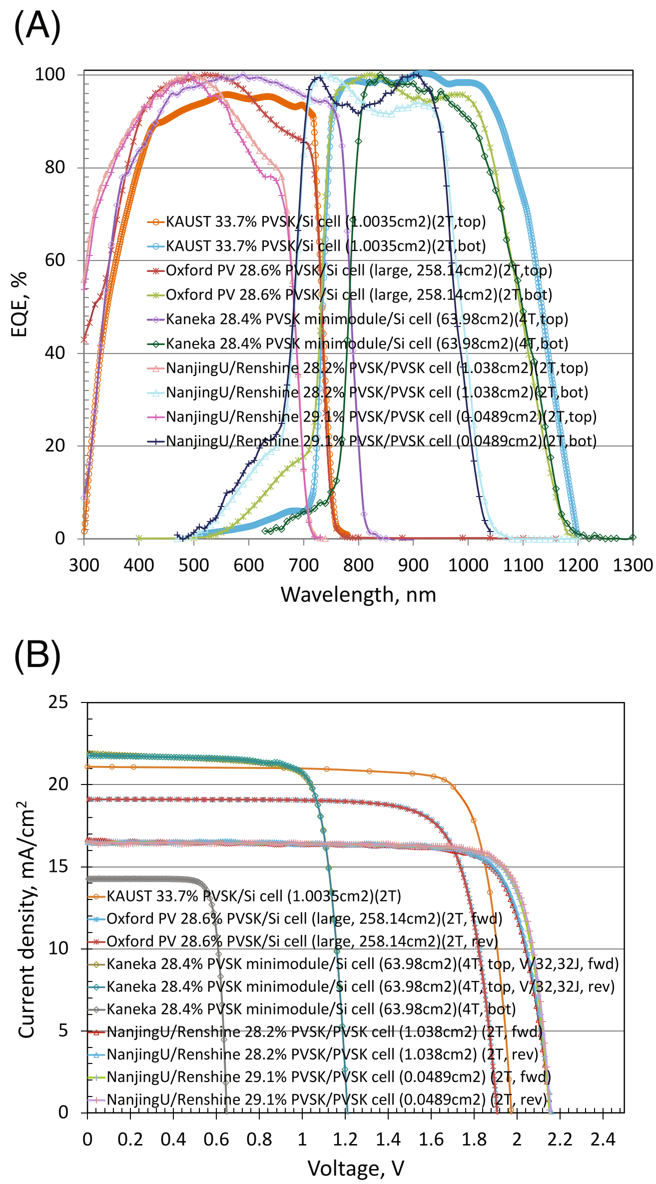

FIGURE 3 (A) External quantum efficiency (EQE) for the new multijunction cell results reported in this issue (most results are normalised). (B) Corresponding current density–voltage (JV) curves.

This cell is only slightly too small to be included in Table 1 as an outright record. The second new result is 22.3% for a smaller 0.4-cm^2 CdTe cell fabricated by First Solar[38] and measured by NREL, displacing one of the table's longest lasting results, a 22.1% cell[1] also fabricated by First Solar in 2015.

The third new result reports a massive improvement in the performance of a CZTSSe cell to 14.9% for a 0.3-cm^2 device fabricated by IoP/CAS[13] and measured by NPVM. The fourth describes an increase in efficiency to 11.4% for pure sulfide, Cd-free, 'earth abundant' Cu_2ZnSnS_4 (CZTS) for a 0.2-cm^2 Cd-free device fabricated by the University of New South Wales, Sydney (UNSW)[39] and again measured by NPVM.

The final three new results in Table 2 relate to the popular perovskite, organic and dye-sensitised cells. An efficiency of 26.0% was measured by JET for a very small 0.07-cm^2 perovskite cell fabricated by the Institute of Semiconductors, Chinese Academy of Sciences (IoS/CAS).[40] An even smaller 0.03-cm^2 organic cell fabricated by Shanghai Jiao Tong University (SJTU) was measured to have 19.2% efficiency[41] by NREL. An earlier result previously overlooked was 13.0% efficiency for a 0.1-cm^2 dye-sensitised cell fabricated by Ecole Polytechnique Fédérale de Lausanne (EPFL)[42] and measured by the Fraunhofer Institute for Solar Energy Systems (FhG-ISE).

This brings us to Table 3, multijunction cells. Accurate measurements of the performance of such cells under standardised test conditions pose additional challenges compared with the case of single junction cells. In particular, for series-connected cells, it is important to have the same current balance between the cells as would occur under the reference spectrum. Standards define a current balance or

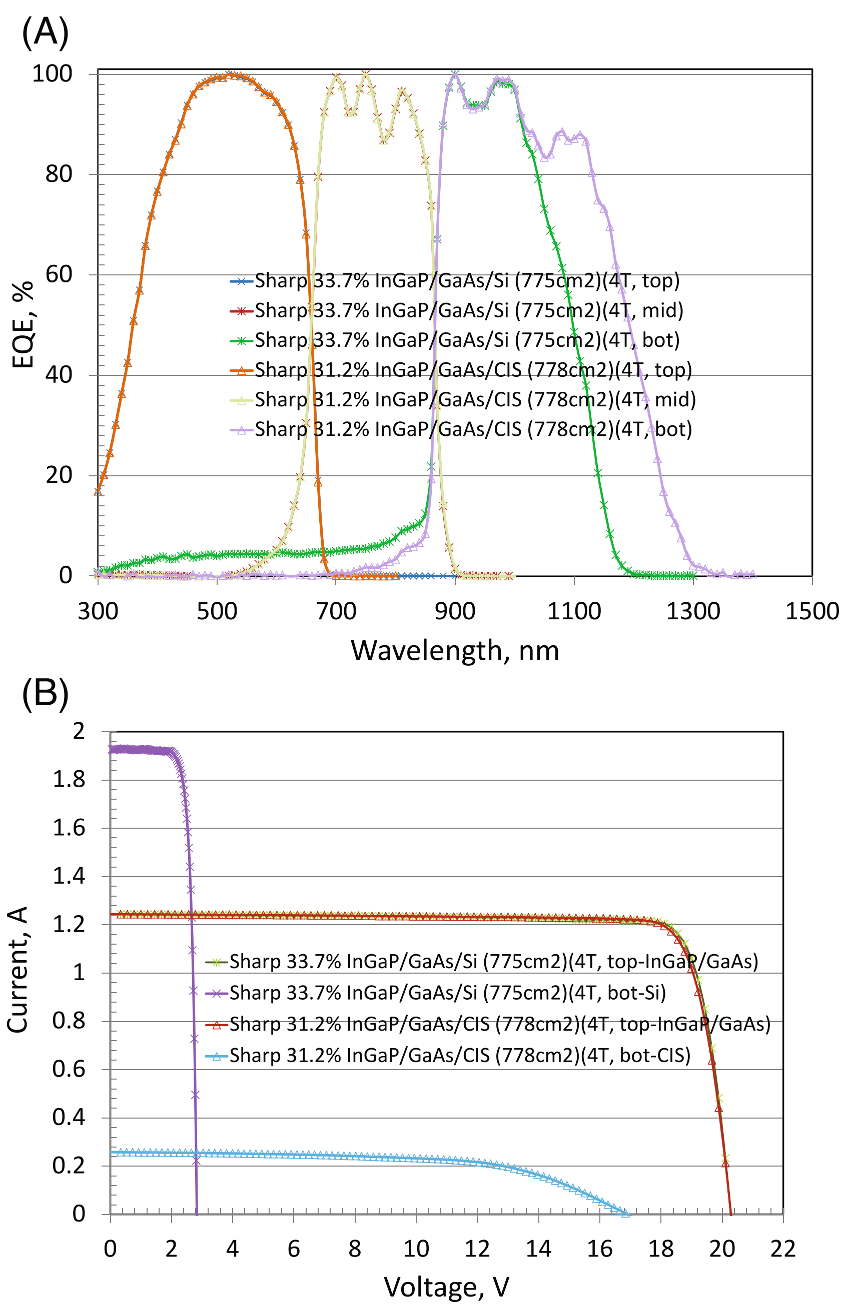

FIGURE 4 (A) External quantum efficiency (EQE) for the new module results reported in this issue (all results are normalised). (B) Corresponding current density–voltage (JV) curves.

matching factor, Z, that estimates how well this is likely to be achieved for each cell under test conditions. Although $Z = 1.00 \pm 0.03$ is regarded as acceptable, the standards encourage striving for $Z = 1.00 \pm 0.01$ to maintain the highest quality of data reported. Our designated test centres have agreed that the tables will only accept results within $Z = 1.00 \pm 0.01$ for the matching factors of multijunction cells in the future, and each will report on Z values when submitting multijunction results.

In the present case, we have five new entries in Table 3, all involving at least one perovskite cell. The first new result is for a 1-cm^2 2-terminal perovskite/silicon tandem cell where there has been remarkable progress since the previous issue of these tables. In that issue, a new record of 31.3% was reported for a cell fabricated by EPFL PVLAB/CSEM and measured by NREL in June 2022, the first to exceed the 30% milestone. This was followed by a 32.5% result later in 2022 for a cell fabricated by Helmholtz-Zentrum Berlin and confirmed by the European Solar Test Installation (ESTI). In March 2023, both ESTI and JET confirmed 33.2% and 33.3%, respectively, for two cells from the same batch fabricated by the King Abdullah University of Science and Technology (KAUST), Saudi Arabia. In May 2023, ESTI confirmed 33.7% efficiency for a cell again fabricated by KAUST.[49] This is higher in efficiency than any other two-cell tandem in the tables.

Also in May, an efficiency of 28.6% was confirmed by FhG-ISE for a much larger 258-cm^2 2-terminal perovskite/silicon tandem cell fabricated by Oxford PV.[50] Good results are also reported for a 64-cm^2 4-terminal tandem fabricated by Kaneka,[51] consisting of a 32-cell perovskite minimodule mechanically stacked onto a single silicon cell. A combined efficiency of 28.4% was measured by the Japanese National Institute of Advanced Industrial Science and Technology (AIST).

The two remaining new results in Table 3 involve a tandem stack of two perovskite cells of different compositions, with both devices fabricated by Nanjing University in collaboration with Renshine Solar (Suzhou) Co. Ltd and both measured by JET. The first is 28.2% efficiency for a 1-cm^2 device,[53] suggesting the 30% milestone is also within reach for this approach, while the second is 29.1% for a much smaller 0.05-cm^2 device.[53]

The final five new results in this issue are in Table 4 (one-sun modules). The first reports an increase in efficiency to 24.7% for a large area (1.8 m^2), monocrystalline silicon module fabricated by Maxeon and measured by NREL. The second reports an efficiency increase to 18.6% for a smaller (810 cm^2) perovskite module fabricated by UtmoLight and measured by JET, while the third reports a substantial increase in efficiency to 13.1% for a larger (1,475 cm^2) module fabricated by Ways Technical Coprporation in conjunction with Nanobit and measured by NREL.

The final two results report two high-efficiency 4-terminal modules fabricated by Sharp and measured by AIST that consist of a III–V tandem cell module mechanically stacked on a silicon module in the first case and a CIGS module in the second case.[70] These are listed as 'notable exceptions' since both are slightly below the Table's 800-cm^2 requirement for classification as a module. The combined efficiency is 33.7% in the first case and 31.2% in the second, suggesting the type of commercial performance the industry might see in the future.

The EQE spectra for the new chalcogenide thin-film and silicon cells and modules reported in the present issue of these tables are shown in Figure 1A, with Figure 1B showing the current density–voltage (JV) curves for the same devices. Figure 2A,B shows the corresponding EQE and JV curves for the new perovskite, organic and dye-sensitised thin-film cell and module results. Figure 3A,B shows these for the new multijunction cell results, while Figure 4A,B shows these for the new 4-terminal multijunction module results.

3 | DISCLAIMER

While the information provided in the tables is provided in good faith, the authors, editors and publishers cannot accept direct responsibility for any errors or omissions.

ACKNOWLEDGEMENTS

The Australian Centre for Advanced Photovoltaics commenced operation in February 2013 with support from the Australian Government through the Australian Renewable Energy Agency (ARENA). The Australian Government does not accept responsibility for the views, information or advice expressed herein. The work at NREL was supported by the U.S. Department of Energy under Contract No. DE-AC36-08-GO28308 with the National Renewable Energy Laboratory. The work at AIST was supported in part by the Japanese New Energy and Industrial Technology Development Organisation (NEDO) under the Ministry of Economy, Trade and Industry (METI). Open access publishing facilitated by University of New South Wales, as part of the Wiley - University of New South Wales agreement via the Council of Australian University Librarians.

DATA AVAILABILITY STATEMENT

The data that support the findings of this study are available from the corresponding author upon reasonable request.

ORCID

Martin A. Green https://orcid.org/0000-0002-8860-396X

REFERENCES

1. Green MA, Dunlop ED, Siefer G, Yoshita M, Kopidakis N, Hao XJ. Solar cell efficiency tables (version 61). *Progr Photovoltaics: Res Appl*. 2022;31(1):3-16. doi:10.1002/pip.3646
2. Green MA, Dunlop ED, Hohl-Ebinger J, et al. Solar cell efficiency tables (version 60). *Progr Photovoltaics: Res Appl*. 2022;30(7):687-701. doi:10.1002/pip.3595
3. Green MA, Emery K, Hishikawa Y, Warta W. Solar cell efficiency tables (version 33). *Progr Photovoltaics: Res Appl*. 2009;17(1):85-94. doi:10.1002/pip.880
4. Yang M, Ru X, Yin S, et al. Over 26% efficiency SHJ solar cells using nano-crystalline silicon layer. In: *Proc. WCPEC-8, Milan*. Paper 1CP.2.2 (2022) (see also: At 26.81%, LONGi sets a new world record

efficiency for silicon solar cells. Press Release, 19 November 2022. https://www.longi.com/en/news/propelling-the-transformation/)
5. Moslehi MM, Kapur P, Kramer J, et al. World-record 20.6% efficiency 156 mm x 156 mm full-square solar cells using low-cost kerfless ultra-thin epitaxial silicon & porous silicon lift-off technology for industry-leading high-performance smart PV modules. In: *PV Asia Pacific Conference (APVIA/PVAP)*. 24 October 2012
6. Keevers MJ, Young TL, Schubert U, Green MA. 10% efficient CSG minimodules. In: *22nd European Photovoltaic Solar Energy Conference, Milan*, September 2007.
7. Kayes BM, Nie H, Twist R, et al. 27.6% conversion efficiency, a new record for single-junction solar cells under 1 sun illumination. In: *Proceedings of the 37th IEEE Photovoltaic Specialists Conference*; 2011.
8. Venkatasubramanian R, O'Quinn BC, Hills JS, et al. 18.2% (AM1.5) efficient GaAs solar cell on optical-grade polycrystalline Ge substrate. In: *Conference Record, 25th IEEE Photovoltaic Specialists Conference, Washington, May 1997*:31-36.
9. Wanlass M. *Systems and Methods for Advanced Ultra-High-Performance InP Solar Cells*. US Patent 9,590,131 B2, 7 March 2017.
10. Nakamura M, Yamaguchi K, Kimoto Y, Yasaki Y, Kato T, Sugimoto H. Cd-free Cu (In,Ga)(Se,S)2 thin-film solar cell with a new world record efficacy of 23.35%. In: *46th IEEE PVSC, Chicago, IL, June 19, 2019*. (see also http://www.solar-frontier.com/eng/news/2019/0117_press.html)
11. Diermann R. *Avancis Claims 19.64% Efficiency for CIGS Module*. PV Magazine International, March 4, 2021. (https://www.pv-magazine.com/2021/03/04/avancis-claims-19-64-efficiency-for-cigs-module/)
12. First Solar Press Release, *First Solar Builds the Highest Efficiency Thin Film PV Cell on Record*, 5 August 2014.
13. Zhou J, Xu X, Wu H, et al. Control of the phase evolution of kesterite by tuning of the selenium partial pressure for solar cells with 13.8% certified efficiency. *Nat Energy*. 2023;8(5):526-535. doi:10.1038/s41560-023-01251-6
14. Yan C, Huang J, Sun K, et al. Cu_2ZnSn S_4 solar cells with over 10% power conversion efficiency enabled by heterojunction heat treatment. *Nat Energy*. 2018;3(9):764-772. doi:10.1038/s41560-018-0206-0
15. Matsui T, Bidiville A, Sai H, et al. High-efficiency amorphous silicon solar cells: impact of deposition rate on metastability. *Appl Phys Lett*. 2015;106(5):053901. doi:10.1063/1.4907001
16. Sai H, Matsui T, Kumagai H, Matsubara K. Thin-film microcrystalline silicon solar cells: 11.9% efficiency and beyond. *Appl Phys Exp*. 2018; 11(2):022301. doi:10.7567/APEX.11.022301
17. Chen W, Zhu Y, Xiu J, et al. Monolithic perovskite/organic tandem solar cells with 23.6% efficiency enabled by reduced voltage losses and optimized interconnecting layer. Nature. *Energy*. 2022;7(3):229-237. doi:10.1038/s41560-021-00966-8
18. Ding B, Yi Zhang Y, Yong Ding Y, et al. Development of efficient and stable perovskite solar cells and modules. In: *Fifth International Conference on Materials & Environmental Science (ICMES-2022)*, June 09–12, 2022, Saïdia, Morocco.
19. Han L, Fukui A, Chiba Y, et al. Integrated dye-sensitized solar cell module with conversion efficiency of 8.2%. *Appl Phys Lett*. 2009; 94(1):013305. doi:10.1063/1.3054160
20. Komiya R, Fukui A, Murofushi N, Koide N, Yamanaka R, Katayama H. Improvement of the conversion efficiency of a monolithic type dye-sensitized solar cell module. In: *Technical Digest, 21st International Photovoltaic Science and Engineering Conference, Fukuoka*, November 2011; 2C-5O-08.
21. Würfel U, Herterich J, List M, et al. A 1 cm^2 organic solar cell with 15.2% certified efficiency: detailed characterization and identification of optimization potential. *Sol RRL*. 2021;5:2000802. doi:10.1002/solr.202000802
22. https://www.pv-magazine.com/2021/03/17/organic-pv-module-with-12-36-efficiency/
23. Accessed November 11, 2019. https://www.encn.de/fileadmin/user_upload/PR_opv-record__.pdf
24. Boyd CC, Cheacharoen R, Leijtens T, McGehee MD. Understanding degradation mechanisms and improving stability of perovskite photovoltaics. *Chem Rev*. 2019;119(5):3418-3451. doi:10.1021/acs.chemrev.8b00336
25. Yang Y, You J. Make perovskite solar cells stable. *Nature*. 2017; 544(7649):155-156. doi:10.1038/544155a
26. Krašovec UO, Bokalič M, Topič M. Ageing of DSSC studied by electroluminescence and transmission imaging. *Solar Energy Mater Solar Cells*. 2013;117:67-72. doi:10.1016/j.solmat.2013.05.029
27. Tanenbaum DM, Hermenau M, Voroshazi E, et al. The ISOS-3 inter-laboratory collaboration focused on the stability of a variety of organic photovoltaic devices. *RSC Adv*. 2012;2(3):882-893. doi:10.1039/C1RA00686J
28. Krebs FC (Ed). *Stability and Degradation of Organic and Polymer Solar Cells*. Wiley; 2012. Jorgensen M, Norrman K, Gevorgyan SA, Tromholt T, Andreasen B, Krebs FC. Stability of polymer solar cells. *Adv Mater*. 2012;24:580-612.
29. Green MA. The passivated emitter and rear cell (PERC): from conception to mass production. *Solar Energy Mater Solar Cells*. 2015;143:190-197. doi:10.1016/j.solmat.2015.06.055
30. Richter A, Benick J, Feldmann F, Fell A, Hermle M, Glunz SW. N-type Si solar cells with passivating electron contact: identifying sources for efficiency limitations by wafer thickness and resistivity variation. *Solar Energy Mater Solar Cells*. 2017;173:96-105. doi:10.1016/j.solmat.2017.05.042
31. Yoshikawa K, Kawasaki H, Yoshida W, et al. Silicon heterojunction solar cell with interdigitated back contacts for a photoconversion efficiency over 26%. *Nat Energy*. 2017;2(5):17032. doi:10.1038/nenergy.2017.32
32. Haase F, Klamt C, Schäfer S, et al. Laser contact openings for local poly-Si-metal contacts enabling 26.1%-efficient POLO-IBC solar cells. *Solar Energy Mater Solar Cells*. 2018;186:184-193. doi:10.1016/j.solmat.2018.06.020
33. Wang Q. Status of crystalline silicon PERC solar cells. In: *NIST/UL Workshop on Photovoltaic Materials Durability, Gaithersburg, MD USA*, Dec 12–13, 2019.
34. https://taiyangnews.info/technology/jinkosolar-record-25-25-efficiency-for-n-type-mono-cell/
35. *LONGi Achieves New World Record for p-Type Solar Cell Efficiency*. Press Release: 20 September 2022. https://www.longi.com/en/news/p-type-hjt-record/
36. *NREL, private communication*, 22 May 2019.
37. https://wwwde.uni.lu/forschung/fstm/dphyms/news_events/physics_colloquium_state_of_the_art_and_future_prospects_of_thin_film_cigs_solar_cells_invited_speaker_prof_marika_edoff_from_uppsala_university
38. First Solar Press Release. *First Solar Achieves Yet Another Cell Conversion Efficiency World Record*, 24 February 2016.
39. Cui X, Sun K, Huang J, et al. Cd-free Cu2ZnSnS4 solar cell with an efficiency greater than 10% enabled by Al2O3 passivation layer. *Energ Environ Sci*. 2019;12(9):2751-2764. doi:10.1039/C9EE01726G
40. https://english.cas.cn/newsroom/research_news/chem/202208/t20220802_310122.shtml
41. Zhu L, Ming Z, Xu J, et al. Single-junction organic solar cells with over 19% efficiency enabled by a refined double-fibril network morphology. *Nat Mater*. 2022;21(6):1-8. doi:10.1038/s41563-022-01244-y
42. Ren Y, Zhang D, Suo J, et al. Hydroxamic acid pre-adsorption raises the efficiency of cosensitized solar cells. *Nature*. 2023;613(7942):60-65. doi:10.1038/s41586-022-05460-z

43. Sasaki K, Agui T, Nakaido K, Takahashi N, Onitsuka R, Takamoto T. *Proceedings, 9th International Conference on Concentrating Photovoltaics Systems, Miyazaki, Japan* 2013.
44. Schygulla P, Müller R, Lackner D, et al. Two-terminal III–V//Si triple-junction solar cell with power conversion efficiency of 35.9% at AM1.5g. *Prog Photovolt Res Appl*. 2022;30(8):869-879. doi:10.1002/pip.3503
45. Essig S, Allebé C, Remo T, et al. Raising the one-sun conversion efficiency of III–V/Si solar cells to 32.8% for two junctions and 35.9% for three junctions. *Nat Energy*. 2017;2:17144. doi:10.1038/nenergy.2017.144
46. Feifel M, Lackner D, Schön J, et al. Epitaxial GaInP/GaAs/Si triple-junction solar cell with 25.9% AM1.5g efficiency enabled by transparent metamorphic $Al_xGa_{1-x}As_yP_{1-y}$ step-graded buffer structures. *Sol RRL*. 2021;5:2000763. doi:10.1002/solr.202000763
47. Grassman TJ, Chmielewski DJ, Carnevale SD, Carlin JA, Ringel SA. $GaAs_{0.75}$ $P_{0.25}$/Si dual-junction solar cells grown by MBE and MOCVD. *IEEE J Photovoltaics*. 2016;6(1):326-331. doi:10.1109/JPHOTOV.2015.2493365
48. Green MA, Keevers MJ, Concha Ramon B, et al. Improvements in sunlight to electricity conversion efficiency: above 40% for direct sunlight and over 30% for global. In: *Paper 1AP.1.2, European Photovoltaic Solar Energy Conference 2015, Hamburg*, September 2015.
49. https://www.kaust.edu.sa/news/kaust-team-sets-world-record-for-tandem-solar-cell-efficiency
50. https://www.oxfordpv.com/oxford-pv-story
51. Yamamoto K, Mishima R, Uzu H, Adachi D. High efficiency perovskite/heterojunction crystalline silicon tandem solar cells: towards industrial-sized cell and module. *Jpn J Appl Phys*. 2023;62(SK):SK1021. doi:10.35848/1347-4065/acc593
52. Jošt M, Köhnen E, Al-Ashouri A, et al. Perovskite/CIGS tandem solar cells: from certified 24.2% toward 30% and beyond. *ACS Energy Lett*. 2022;7(4):1298-1307. doi:10.1021/acsenergylett.2c00274
53. Lin R, Xu J, Wei MY, et al. All-perovskite tandem solar cells with improved grain surface passivation. *Nature*. 2022;603(7899):73-78. doi:10.1038/s41586-021-04372-8
54. Xiao K, Lin YH, Zhang M, et al. Scalable processing for realizing 21.7%-efficient all-perovskite tandem solar modules. *Science*. 2022;376(6594):762-767. doi:10.1126/science.abn7696
55. Sai H, Matsui T, Koida T, Matsubara K. Stabilized 14.0%-efficient triple-junction thin-film silicon solar cell. *Appl Phys Lett*. 2016;109:183506. doi:10.1063/1.49669996
56. Matsui T, Maejima K, Bidiville A, et al. High-efficiency thin-film silicon solar cells realized by integrating stable a-Si:H absorbers into improved device design. *Jpn J Appl Phys*. 2015;54:08KB10. doi:10.7567/JJAP.54.08KB10
57. Accessed 28 October 2018. http://mldevices.com/index.php/news/
58. Geisz JF, Steiner MA, Jain N, et al. Building a six-junction inverted metamorphic concentrator solar cell. *IEEE J Photovoltaics*. 2018;8(2):626-632. doi:10.1109/JPHOTOV.2017.2778567
59. Makita K, Kamikawa Y, Mizuno H, et al. III-V//$Cu_xIn_{1-y}Ga_ySe_2$ multijunction solar cells with 27.2% efficiency fabricated using modified smart stack technology with Pd nanoparticle array and adhesive material. *Prog Photovolt Res Appl*. 2021;29:887-898. doi:10.1002/pip.3398
60. Chen W, Zhu YD, Xiu JW, et al. Monolithic perovskite/organic tandem solar cells with 23.6% efficiency enabled by reduced voltage losses and optimized interconnecting layer. *Nat Energy*. 2022;7:229-237. doi:10.1038/s41560-021-00966-8
61. Accessed 28 October 2019. https://www.hanwha-qcells.com
62. Mattos LS, Scully SR, Syfu M, Olson E, Yang L, Ling C, Kayes BM, He G. New module efficiency record: 23.5% under 1-sun illumination using thin-film single-junction GaAs solar cells. *Proceedings of the 38th IEEE Photovoltaic Specialists Conference*, 2012.
63. Sugimoto H. High efficiency and large volume production of CIS-based modules. In: *40th IEEE Photovoltaic Specialists Conference*, Denver, June 2014.
64. Accessed 28 October 2019. http://www.firstsolar.com/en-AU/-/media/First-Solar/Technical-Documents/Series-6-Datasheets/Series-6-Datasheet.ashx
65. Cashmore JS, Apolloni M, Braga A, et al. Improved conversion efficiencies of thin-film silicon tandem (MICROMORPH ™) photovoltaic modules. *Solar Energy Mater Solar Cells*. 2016;144:84-95. doi:10.1016/j.solmat.2015.08.022
66. https://taiyangnews.info/markets/china-pv-news-snippets-361/
67. http://www.waystech.net/zh-tw/service/index/finishing_center
68. *Sharp Achieves World's Highest[*1] Conversion Efficiency of 32.65%[*2] in a Lightweight, Flexible, Practically Sized Solar Module*. Press Release: June 6, 2022. https://global.sharp/corporate/news/220606-a.html
69. Bheemreddy V, Liu BJJ, Wills A, Murcia CP. Life prediction model development for flexible photovoltaic modules using accelerated damp heat testing. In: *IEEE 7th World Conf. on Photovoltaic Energy Conversion (WCPEC)*; 2018:1249-1251.
70. Takamoto T, Juso H, Ueda K, et al. IMM triple-junction solar cells and modules optimized for space and terrestrial conditions. In: *Proceedings of the 44th IEEE Photovoltaic Specialist Conference (PVSC)*; 2017. doi:10.1109/PVSC.2017.8366097
71. Slade A, Garboushian V. 27.6% efficient silicon concentrator cell for mass production. In: *Technical Digest, 15th International Photovoltaic Science and Engineering Conference, Shanghai, October 2005*:701.
72. Ward JS, Ramanathan K, Hasoon FS, et al. A 21.5% efficient cu (in, Ga)Se2 thin-film concentrator solar cell. *Progr Photovoltaics: Res Appl*. 2002;10(1):41-46. doi:10.1002/pip.424
73. Dimroth F, Tibbits TND, Niemeyer M, et al. Four-junction wafer-bonded concentrator solar cells. *IEEE J Photovoltaics*. 2016;6(1):343-349. doi:10.1109/JPHOTOV.2015.2501729
74. NREL. *Press Release NR-4514*, 16 December 2014.
75. *Press Release, Sharp Corporation*, 31 May 2012 (accessed at http://sharp-world.com/corporate/news/120531.html on 5 June 2013).
76. Jain N, Schulte KL, Geisz JF, et al. High-efficiency inverted metamorphic 1.7/1.1 eV GaInAsP/GaInAs dual-junction solar cells. *Appl Phys Lett*. 2018;112(5):053905. doi:10.1063/1.5008517
77. Steiner M, Siefer G, Schmidt T, Wiesenfarth M, Dimroth F, Bett AW. 43% sunlight to electricity conversion efficiency using CPV. *IEEE J Photovoltaics*. 2016;6(4):1020-1024. doi:10.1109/JPHOTOV.2016.2551460
78. Green MA, Keevers MJ, Thomas I, Lasich JB, Emery K, King RR. 40% efficient sunlight to electricity conversion. *Progr Photovoltaics: Res Appl*. 2015;23(6):685-691. doi:10.1002/pip.2612
79. Chiang CJ, Richards EH. A 20% efficient photovoltaic concentrator module. In: *Conf. Record, 21st IEEE Photovoltaic Specialists Conference, Kissimimee*, May 1990: 861-863.
80. http://amonix.com/pressreleases/amonix-achieves-world-record-359-module-efficiency-rating-nrel-4 (accessed 23 October 2013).
81. van Riesen S, Neubauer M, Boos A, et al. New module design with 4-junction solar cells for high efficiencies. In: *Proceedings of the 11th Conference on Concentrator Photovoltaic Systems*; 2015.
82. Martínez JF, Steiner M, Wiesenfarth M, Siefer G, Glunz SW, Dimroth F. Power rating procedure of hybrid CPV/PV bifacial modules. *Prog Photovolt Res Appl*. 2021;29(6):614-629. doi:10.1002/pip.3410
83. Zhang F, Wenham SR, Green MA. Large area, concentrator buried contact solar cells. *IEEE Trans Electron Devices*. 1995;42(1):144-149. doi:10.1109/16.370024
84. Slooff LH, Bende EE, Burgers AR, et al. A luminescent solar concentrator with 7.1% power conversion efficiency. *Phys Stat sol (RRL)*. 2008;2(6):257-259. doi:10.1002/pssr.200802186

85. Steiner M, Wiesenfarth M, Martínez JF, Siefer G, Dimroth F. Pushing energy yield with concentrating photovoltaics. *AIP Conf Proc*. 2019;2149:060006. doi:10.1063/1.5124199
86. Müllejans H, Winter S, Green MA, Dunlop ED. What is the correct efficiency for terrestrial concentrator PV devices? In: *38th European Photovoltaic Solar Energy Conference*; 2021. (accepted for presentation)
87. Gueymard CA, Myers D, Emery K. Proposed reference irradiance spectra for solar energy systems testing. *Solar Energy*. 2002;73(6):443-467. doi:10.1016/S0038-092X(03)00005-7

How to cite this article: Green MA, Dunlop ED, Yoshita M, et al. Solar cell efficiency tables (version 62). *Prog Photovolt Res Appl*. 2023;31(7):651-663. doi:10.1002/pip.3726

APPENDIX A: LIST OF DESIGNATED TEST CENTRES

A list of designated test centres can be found in version 61.[1] An additional designated test centre not there listed is:

Newport PV Lab
3050 North 300 West, North Logan, UT 84341, USA.
Contact: Paulette Frischknecht
Office: +1435–753-3729
Email: paulette.frischknecht@mksinst.com
(Terrestrial cells)